The Treatment of Discontinuities in Computing the Nonlinear Energy Transfer for Finite-Depth Gravity Wave Spectra

RICHARD M. GORMAN

National Institute of Water and Atmospheric Research, Hamilton, New Zealand

(Manuscript received 29 August 2001, in final form 5 June 2002)

ABSTRACT

The calculation of nonlinear energy transfer between interacting waves is one of the most computationally demanding tasks in understanding the dynamics of the growth and transformation of wind-generated surface waves. For shallow water in particular, existing schemes for computing the full Boltzmann integral representing the nonlinear energy transfer rate converge slowly with increasing spectral resolution. This means that it is difficult to build a spectral wave model with a treatment of nonlinear interactions that is sufficiently accurate without being computationally prohibitive for practical simulations. This paper examines the behavior of terms in the Boltzmann integral with a view to identifying potential improvements in numerical methods used in its solution. Discontinuities are identified in the variation of the nonlinear interaction coefficient where quadruplets of interacting wavenumbers include pairwise matches ($\mathbf{k}_1 = \mathbf{k}_3$, $\mathbf{k}_2 = \mathbf{k}_4$) or ($\mathbf{k}_1 = \mathbf{k}_4$, $\mathbf{k}_2 = \mathbf{k}_3$), a generalization of the specific case $\mathbf{k}_1 = \mathbf{k}_2 = \mathbf{k}_3 = \mathbf{k}_4$ noted in earlier works. The discontinuities are not present in the deep-water case and increase in magnitude with decreasing water depth. The behavior of the interaction coefficient in their vicinity is described, and their role in limiting the accuracy of the integration procedure is considered. It is found that the discontinuities are removed when the interacting wavenumbers are constrained to satisfy the resonance conditions. Because of the asymmetrical structure of the action product term, these discontinuities should not directly cause significant errors in existing algorithms for computing nonlinear transfer rates. Indeed, the kernel of the Boltzmann integral vanishes at these points.

1. Introduction

During the growth of wind-generated waves on the ocean surface, the evolution of the shape of the wave spectrum is largely controlled by the transfer of energy between frequency bands resulting from nonlinear wave–wave interactions (Hasselmann et al. 1973). A spectral wave model that attempts to describe the process of wave transformation from physical principles will require an accurate representation of this mechanism, accounting for energy transfers between all resonant four-wave combinations. The computational complexity of this term means, however, that a full and accurate solution is difficult to achieve in practical model applications. Hence a much-simplified approach is often used, such as the discrete interaction approximation (Hasselmann et al. 1985) employed for example in both the Wave Model (WAM) (Hasselmann et al. 1988) and the shallow-water Simulating Waves Nearshore (SWAN) model (Booij et al. 1999; Holthuijsen et al. 1993; Ris et al. 1999). This reduced method has shown difficulties providing an accurate representation of nonlinear transfer, especially in shallow water (Gorman and Neilson 1999), and there remains a need to develop nonlinear interaction algorithms that are both fast and accurate.

To this end, algorithms have been sought for a near-exact solution of the Boltzmann integral. Several methods of improving the efficiency of solution have been identified in the deep-water case (Komatsu and Masuda 1996; Masuda 1980; Resio and Perrie 1991; Webb 1978). For arbitrary depth, the EXACT-NL model originally developed by Hasselmann and Hasselmann (1985) and extended by Thacker (1982) and Snyder et al. (1993) can be used. An efficient piecewise-linear discretization and high use of symmetries allows EXACT-NL to integrate the interaction strength over the space of interacting wavenumbers with a numerical cost acceptable for single point applications, though still problematic for application in an extended spatial domain. The main limiting factor found was that before adequate convergence could be achieved, a much higher internal resolution was needed for the integration than was needed simply to represent the wave spectrum. Other finite-depth computation methods have been developed by Resio et al. (2001) and by Hashimoto et al.

Corresponding author address: Dr. Richard M. Gorman, National Institute of Water and Atmospheric Research, P.O. Box 11-115, Hamilton, New Zealand.
E-mail: r.gorman@niwa.co.nz

(1998). The latter describe an alternative integration procedure, extending the Masuda (1980) algorithm to shallow water, which also found poorer convergence properties than for the deep-water limit. These results suggest that a closer investigation of possible singular points or discontinuities in the variation of the interaction strength is needed.

2. The Boltzmann integral for nonlinear wave–wave interactions

Spectral wave models describe the wave field by an action density $N(\mathbf{k}, \mathbf{x}, t)$ representing the amount of variance associated with wavenumber vector $\mathbf{k}$ at position $\mathbf{x}$ and time t (see appendix). The rate of change of the action density N is described by a radiative transfer equation, which may be summarized as

$$\frac{\partial N}{\partial t} + P = S_{\ln} + S_{\mathrm{nl4}} + S_{\mathrm{nl3}} + S_{\mathrm{diss}} + \cdots, \quad (1)$$

where P represents propagation, and the source terms S_{in}, S_{nl4}, S_{nl3}, and S_{diss}, respectively, represent source terms for the physical processes of energy input from wind stress, four-wave and three-wave nonlinear interactions, and whitecap dissipation. Other physical processes can be represented by additional source terms as required. At our present state of knowledge, the nonlinear interactions are unique among these source terms in that they are in principle calculable from physical laws without recourse to empirical parameterization, albeit with some approximation being needed.

The nonlinear interactions can be decomposed for computational purposes into three-wave and four-wave interactions, being the leading terms of a weakly nonlinear approximation (Hasselmann 1962; Zakharov 1999). The former become significant in shallow water, and a separate treatment of this term can be included in a spectral model for shallow-water applications. The SWAN shallow-water spectral model (Booij et al. 1999; Ris et al. 1999), for example, has separate subroutines for three-wave and four-wave interactions, based on this split. But we shall not discuss the calculation of three-wave interactions in the present work, being solely concerned with computational aspects of the four-wave part of the interaction. In effect, we are concerned with the limited but practical task of improving the accuracy and efficiency of the subroutines used to compute S_{nl4} in existing models, putting aside for the time being any shortcomings in the computation of S_{nl3} and other source terms, or indeed in the theoretical formulation of the models.

Hasselmann (1962) used a perturbation analysis to derive the transfer rate to and from a spectral component arising from interactions with sets of three other spectral components. The resulting source term takes the form of a Boltzmann integral over the phase space of interacting quadruplets:

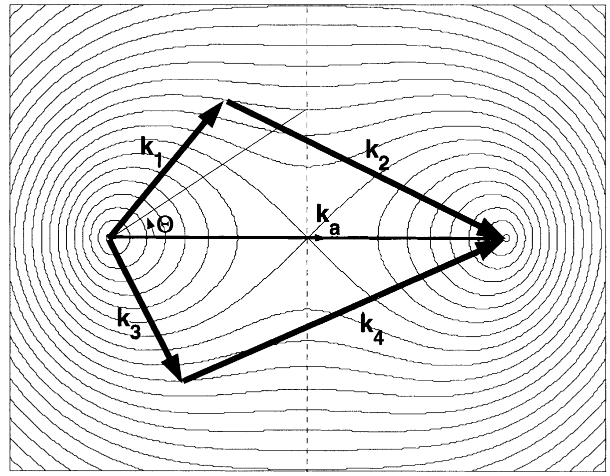

FIG. 1. Chart showing interacting wavenumber vectors, and contour lines on which the wavenumber condition $\mathbf{k}_1 + \mathbf{k}_2 = \mathbf{k}_a = \mathbf{k}_3 + \mathbf{k}_4$ is satisfied, and $\omega_1 + \omega_2 = \omega_3 + \omega_4$ is constant. The minimum angle Θ for the orientation of wavenumbers $\mathbf{k}_1$ in the half-space $|\mathbf{k}_1| \le |\mathbf{k}_2|$ is marked. In this example, a depth $h = 10$ m was used.

$$\begin{aligned} S_{\mathrm{nl4}}(\mathbf{k}_4) = \int & d\mathbf{k}_1\, d\mathbf{k}_2\, d\mathbf{k}_3 G(\mathbf{k}_1, \mathbf{k}_2, \mathbf{k}_3, \mathbf{k}_4) \\ & \times [N_1 N_2 (N_3 + N_4) - N_3 N_4 (N_1 + N_2)] \\ & \times \delta(\mathbf{k}_1 + \mathbf{k}_2 - \mathbf{k}_3 - \mathbf{k}_4) \\ & \times \delta(\omega_1 + \omega_2 - \omega_3 - \omega_4), \end{aligned} \quad (2)$$

where the $N_i = N(\mathbf{k}_i, \mathbf{x}, t)$ are the action densities at each of the interacting wavenumber vectors $\mathbf{k}_i$ (with corresponding angular frequency ω_i), ρ is water density, g is gravitational acceleration, and

$$G(\mathbf{k}_1, \mathbf{k}_2, \mathbf{k}_3, \mathbf{k}_4) = \frac{9\pi g^2 D^2(\mathbf{k}_1, \mathbf{k}_2, \mathbf{k}_3, \mathbf{k}_4)}{4\rho^2 \omega_1 \omega_2 \omega_3 \omega_4} \quad (3)$$

incorporates an interaction coefficient $D(\mathbf{k}_1, \mathbf{k}_2, \mathbf{k}_3, \mathbf{k}_4)$. The Dirac delta functions in the integral (2) select the resonance conditions

$$\mathbf{k}_1 + \mathbf{k}_2 - \mathbf{k}_3 - \mathbf{k}_4 = 0 \quad \text{and} \quad (4)$$

$$\omega_1 + \omega_2 - \omega_3 - \omega_4 = 0, \quad (5)$$

which are associated with conservation of momentum and energy in the interaction (Hasselmann 1963). The combinations of wavenumbers that satisfy these conditions can be illustrated by the interaction diagram (Fig. 1), originally devised by Longuet–Higgins (1976). In this, for a given pair $(\mathbf{k}_3, \mathbf{k}_4)$, the combinations of $(\mathbf{k}_1, \mathbf{k}_2)$, which satisfy (4) and (5), will all lie on the same contour of frequency sum $\omega_1 + \omega_2 = \omega_3 + \omega_4$ as $(\mathbf{k}_3, \mathbf{k}_4)$.

A method for evaluating the Boltzmann integral (2) has been described for the deep-water case by Masuda (1980) and extended to shallow water by Hashimoto et al. (1998). They first note that symmetry between $\mathbf{k}_1$ and $\mathbf{k}_2$ allows the integral domain to be restricted to the half-space in which the magnitude $k_1(\equiv|\mathbf{k}_1|) \le k_2$. They then make use of the wavenumber delta function to integrate over $\mathbf{k}_2$, and transform from wavenumber coordinates to frequency and direction coordinates $\{\omega_3, \theta_3, \omega_1, \theta_1\}$ using

$$\frac{\Phi(\omega, \theta)}{\omega} d\omega d\theta = N(\mathbf{k}) d\mathbf{k}. \quad (6)$$

This allows the frequency delta function to be absorbed by the ω_1 integration, giving the result

$$\begin{aligned}\frac{\partial\Phi(\omega_4, \theta_4)}{\partial t} &= \frac{2\omega_4 k_4}{C_g(k_4)} \int d\theta_3 \int d\omega_3 \int d\theta_1 \left[\frac{k_1 k_3}{C_g(k_1)C_g(k_3)} \frac{G}{S}\right] \\ &\quad \times [N_1 N_2(N_3 + N_4) - N_3 N_4(N_1 + N_2)], \end{aligned} \quad (7)$$

where $C_g(k)$ is the group velocity

$$C_g(k) = \frac{\partial\omega}{\partial k} = \frac{1}{2}\left(1 + \frac{2kh}{\sinh 2kh}\right)\sqrt{\frac{g}{k}\tanh kh}. \quad (8)$$

Making use of symmetry, the integration range of the direction θ_1 is

$$\Theta = \cos^{-1}\left(\frac{k_a}{2k_1}\right) \le |\theta_1 - \theta_a| \le \pi \quad (9)$$

relative to the direction of $\mathbf{k}_a = \mathbf{k}_3 + \mathbf{k}_4$ (see Fig. 1). The denominator S arises from the frequency delta function, as follows. For arbitrary functions F and g,

$$\int dx F(x)\delta[g(x)] = \left.\frac{F}{|\partial g/\partial x|}\right|_{g(x)=0}. \quad (10)$$

Now the ω_2 term in the frequency delta function has an implicit dependence on ω_1 after the wavenumber delta function has been applied to force $\mathbf{k}_2 = \mathbf{k}_3 + \mathbf{k}_4 - \mathbf{k}_1$. Hence we get a derivative term in the denominator:

$$\begin{aligned} S &= \left|\frac{\partial}{\partial\omega_1}(\omega_1 + \omega_2(\omega_1) - \omega_3 - \omega_4)\right| \\ &= \left|1 + \frac{C_g(k_2)}{C_g(k_1)}\left\{\frac{k_1 - k_a\cos(\theta_1 - \theta_a)}{k_2}\right\}\right| \\ &= \left|1 - \frac{C_g(k_2)}{C_g(k_1)}\cos(\theta_2 - \theta_1)\right|. \end{aligned} \quad (11)$$

With the integration domain limited to the half-space $k_1 \le k_2$, S vanishes only when $\mathbf{k}_1 = \mathbf{k}_2 = ½\mathbf{k}_a$.

Masuda (1980) and Hashimoto et al. (1998) describe a procedure to carry out the integration that includes a convergent treatment of the behavior of S around the singular point. When applied to representative spectra of the Joint North Sea Wave Project (JONSWAP) and Pierson–Moskowitz form, all three sets of authors found that the nonlinear transfer can be computed smoothly and accurately in deep-water conditions, even with a relatively coarse mesh (24 × 36) in frequency and direction. Extending the Masuda (1980) deep-water method to finite depth, Hashimoto et al. (1998) found that the calculation became unstable with this coarse resolution. Even with a 72 × 96 mesh, the computed nonlinear energy transfer had a ''zigzag'' shape, with possibly spurious fine structure particularly evident in the frequency band above the peak where S_{nl4} is negative. This behavior was especially notable where the peak wavenumber k_p is of order $k_p h \approx 1$. Similar features have been noted in nonlinear transfers computed by Snyder et al. (1993).

3. Structure of the interaction coefficient

The interaction coefficient D was derived by Hasselmann (1962), and re-expressed in corrected form by Herterich and Hasselmann (1980). An alternative formulation has also been presented by Zakharov (1999) to which the following analysis could equally be applied. Noting that Resio et al. (2001) have found the two formulations to be numerically equivalent, we would expect similar results. The Herterich and Hasselmann (1980) form of the interaction coefficient is

$$D = \frac{1}{3}(D^{++-}_{\mathbf{k}_1\mathbf{k}_2-\mathbf{k}_3} + D^{+-+}_{\mathbf{k}_2-\mathbf{k}_3\mathbf{k}_1} + D^{-++}_{-\mathbf{k}_3\mathbf{k}_1\mathbf{k}_2}), \quad (12)$$

where

$$\begin{aligned} D^{s_1 s_2 s_3}_{\mathbf{k}_1\mathbf{k}_2\mathbf{k}_3} &= \frac{iD^{s_2 s_3}_{\mathbf{k}_2\mathbf{k}_3}}{\omega^2_{\mathbf{k}_2+\mathbf{k}_3} - (\omega_2 + \omega_3)^2}\left\{2(\omega_1 + \omega_2 + \omega_3)\left(\frac{\omega_1^2\omega^2_{\mathbf{k}_2+\mathbf{k}_3}}{g^2} - \mathbf{k}_1\cdot(\mathbf{k}_2 + \mathbf{k}_3)\right) - \frac{\omega_1|\mathbf{k}_2 + \mathbf{k}_3|^2}{\cosh^2|\mathbf{k}_2 + \mathbf{k}_3|h} - \frac{(\omega_2 + \omega_3)k_1^2}{\cosh^2 k_1 h}\right\} \\ &\quad - iD^{s_2 s_3}_{\mathbf{k}_2\mathbf{k}_3}\frac{\omega_1}{g^2}(\omega_1^2 + \omega^2_{\mathbf{k}_2+\mathbf{k}_3}) + E^{s_2 s_3}_{\mathbf{k}_2\mathbf{k}_3}\left[\frac{\omega_1^3(\omega_2 + \omega_3)}{g} - g\mathbf{k}_1\cdot(\mathbf{k}_2 + \mathbf{k}_3) - \frac{gk_1^2}{\cosh^2 k_1 h}\right] \\ &\quad + \frac{\omega_1}{2g^2}(\mathbf{k}_2\cdot\mathbf{k}_3)[(\omega_1 + \omega_2 + \omega_3)(\omega_2^2 + \omega_3^2) + \omega_2\omega_3(\omega_2 + \omega_3)] - \frac{\omega_1\omega_2^2 k_3^2}{2g^2}(\omega_1 + \omega_2 + 2\omega_3) \end{aligned}$$

$$- \frac{\omega_1 \omega_3^2 k_2^2}{2g^2}(\omega_1 + 2\omega_2 + \omega_3) \tag{13}$$

$$D^{s_2 s_3}_{\mathbf{k}_2 \mathbf{k}_3} = i(\omega_2 + \omega_3)[k_2 k_3 \tanh(k_2 h)\tanh(k_3 h) - \mathbf{k}_2 \cdot \mathbf{k}_3] - \frac{i}{2}\left(\frac{\omega_2 k_3^2}{\cosh^2 k_3 h} + \frac{\omega_3 k_2^2}{\cosh^2 k_2 h}\right) \tag{14}$$

$$E^{s_2 s_3}_{\mathbf{k}_2 \mathbf{k}_3} = \frac{1}{2g}\left[\mathbf{k}_2 \cdot \mathbf{k}_3 - \frac{\omega_2 \omega_3}{g^2}(\omega_2^2 + \omega_3^2 + \omega_2 \omega_3)\right], \tag{15}$$

and we have used the notation

$$\omega_i = s_i \omega_{\mathbf{k}_i}, \qquad s_i = \pm 1 \tag{16}$$

$$\omega_{\mathbf{k}} = \sqrt{gk \tanh kh}, \qquad k = |\mathbf{k}|. \tag{17}$$

Herterich and Hasselmann (1980) have noted that D has a discontinuity at the point $\mathbf{k}_1 = \mathbf{k}_2 = \mathbf{k}_3 = \mathbf{k}_4$. For wavenumbers arbitrarily close to this point, the limiting value near the discontinuity varies through a finite range as a function of the direction from which the point is approached. Herterich and Hasselmann (1980) discuss the effect that this will be expected to have in computing the nonlinear transfer rate. They estimate that ignoring the discontinuity in computations with a narrow-peaked approximation would produce a negligible error for $k_p h \geq 0.7$ and $k_p h \leq 0.3$, but that this error could be considerable for $k_p h \approx 0.5$.

It has not been widely noted, however, that this behavior actually extends to the more general cases ($\mathbf{k}_1 = \mathbf{k}_3$, $\mathbf{k}_2 = \mathbf{k}_4$), ($\mathbf{k}_1 = \mathbf{k}_4$, $\mathbf{k}_2 = \mathbf{k}_3$), $\mathbf{k}_1 = 0$ and $\mathbf{k}_2 = 0$. It arises when the denominator vanishes in the first term of $D^{s_1 s_2 s_3}_{\mathbf{k}_1 \mathbf{k}_2 \mathbf{k}_3}$. The numerator also goes to zero in this limit, leaving a direction-dependent limiting behavior noted above. To illustrate this, consider the behavior of the first term $D^{+ + -}_{\mathbf{k}_1 \mathbf{k}_2 - \mathbf{k}_3}$ in (12) when $\mathbf{q} = \mathbf{k}_2 - \mathbf{k}_3$ is small. The magnitude of $\mathbf{k}_2$ will be given by

$$k_2^2 = k_3^2 + 2qk_3 \cos\theta_{q3} + q^2, \tag{18}$$

where $\theta_{qi} = \theta_q - \theta_i$ is the angle between $\mathbf{q}$ and $\mathbf{k}_i$ (for $i = 1, 2, 3, 4$). Some other expressions we will use are

$$\mathbf{k}_2 \cdot \mathbf{k}_3 = k_3^2 + qk_3 \cos\theta_{q3}, \tag{19}$$

$$k_2 = k_3 + q\cos\theta_{q3} + O(q^2), \tag{20}$$

$$\omega_2 = \omega_3 + C_g(k_3) q \cos\theta_{q3} + O(q^2), \quad \text{and} \tag{21}$$

$$\omega^2_{\mathbf{k}_2 - \mathbf{k}_3} = gq \tanh qh. \tag{22}$$

We can write the first term of (12) as

$$D^{+ + -}_{\mathbf{k}_1 \mathbf{k}_2 - \mathbf{k}_3} = \frac{iD^{+ -}_{\mathbf{k}_2 - \mathbf{k}_3}}{A}\{B\} - iD^{+ -}_{\mathbf{k}_2 - \mathbf{k}_3} C + E^{+ -}_{\mathbf{k}_2 - \mathbf{k}_3} F + G, \tag{23}$$

and consider each component in turn. The denominator can be expanded as

$$\begin{aligned} A &= \omega_{\mathbf{q}}^2 - (\omega_2 - \omega_3)^2 \\ &= gq \tan qh - [C_g(k_3) q \cos\theta_{q3} + O(q^2)]^2. \end{aligned} \tag{24}$$

For the other terms, after using the dispersion relation (17) to re-express the hyperbolic functions, we can expand in powers of q to find

$$\begin{aligned} iD^{+ -}_{\mathbf{k}_2 - \mathbf{k}_3} &= -(\omega_2 - \omega_3)\left(\frac{\omega_2^2 \omega_3^2}{g^2} + \mathbf{k}_2 \cdot \mathbf{k}_3\right) + \frac{1}{2}\left[\omega_2\left(k_3^2 - \frac{\omega_3^4}{g^2}\right) - \omega_3\left(k_2^2 - \frac{\omega_2^4}{g^2}\right)\right] \\ &= q\cos\theta_{q3}\left\{-\frac{1}{2}C_g(k_3)\left[k_3^2 - \frac{\omega_3^4}{g^2}\right] - \omega_3 k_3\right\} + O(q^2). \end{aligned} \tag{25}$$

$$\begin{aligned} B &= 2(\omega_1 + \omega_2 - \omega_3)\left[\frac{\omega_1^2 \omega^2_{\mathbf{k}_2 - \mathbf{k}_3}}{g^2} - \mathbf{k}_1 \cdot (\mathbf{k}_2 - \mathbf{k}_3)\right] - \omega_1\left(|\mathbf{k}_2 - \mathbf{k}_3|^2 - \frac{\omega^4_{\mathbf{k}_2 - \mathbf{k}_3}}{g^2}\right) - (\omega_2 - \omega_3)\left(k_1^2 - \frac{\omega_1^4}{g^2}\right) \\ &= 2[\omega_1 + C_g(k_3) q \cos\theta_{q3} + O(q^2)]\left(\frac{\omega_1^2 q^2 gh}{g^2} - k_1 q \cos\theta_{q1}\right) - \omega_1[q^2 - O(q^4)] \\ &\quad - [C_g(k_3) q \cos\theta_{q3} + O(q^2)]\left(k_1^2 - \frac{\omega_1^4}{g^2}\right) \\ &= q\left\{-2\omega_1 k_1 \cos\theta_{q1} - C_g(k_3)\cos\theta_{q3}\left[k_1^2 - \frac{\omega_1^4}{g^2}\right] + 2\frac{\omega_1^3}{g}\tanh qh\right\} + O(q^2) \end{aligned} \tag{26}$$

$$C = \frac{\omega_1}{g^2}(\omega_1^2 + \omega_{\mathbf{k}_2-\mathbf{k}_3}^2) = \frac{\omega_1}{g^2}(\omega_1^2 + qg \tanh qh) \tag{27}$$

$$E_{\mathbf{k}_2-\mathbf{k}_3}^{+\ -} = \frac{1}{2g}\left[-\mathbf{k}_2 \cdot \mathbf{k}_3 + \frac{\omega_2\omega_3}{g^2}(\omega_2^2 + \omega_3^2 - \omega_2\omega_3)\right] = \frac{1}{2g}\left\{-\left(k_3^2 - \frac{\omega_3^4}{g^2}\right) + \left[2\frac{\omega_3^2}{g^2}C_g(k_3) - k_3\right]q\cos\theta_{q3} + O(q^2)\right\} \tag{28}$$

$$\begin{aligned} F &= \left[\frac{\omega_1^3(\omega_2 - \omega_3)}{g} - g\mathbf{k}_1 \cdot (\mathbf{k}_2 - \mathbf{k}_3) - g\left(k_1^2 - \frac{\omega_1^4}{g^2}\right)\right] \\ &= -g\left(k_1^2 - \frac{\omega_1^4}{g^2}\right) + q\left[\frac{\omega_1^3}{g}C_g(k_3)\cos\theta_{q3} - gk_1\cos\theta_{q1}\right] + O(q^2) \end{aligned} \tag{29}$$

$$\begin{aligned} G &= \frac{\omega_1}{2g^2}(-\mathbf{k}_2 \cdot \mathbf{k}_3)[(\omega_1 + \omega_2 - \omega_3)(\omega_2^2 + \omega_3^2) - \omega_2\omega_3(\omega_2 - \omega_3)] - \frac{\omega_1\omega_2^2k_3^2}{2g^2}(\omega_1 + \omega_2 - 2\omega_3) \\ &\quad - \frac{\omega_1\omega_3^2k_2^2}{2g^2}(\omega_1 + 2\omega_2 - \omega_3) = -2k_3^2\frac{\omega_1^2\omega_3^2}{g^2} + O(q). \end{aligned} \tag{30}$$

Hence, the whole term has a limiting form for small q of

$$\begin{aligned} D_{\mathbf{k}_1\mathbf{k}_2-\mathbf{k}_3}^{+\ +\ -} \xrightarrow[q\to 0]{} & \frac{2\cos\theta_{q3}\left[\omega_3k_3 + \frac{1}{2}C_g(k_3)\left(k_3^2 - \frac{\omega_3^4}{g^2}\right)\right]\left[\omega_1k_1\cos\theta_{q1} + \frac{1}{2}C_g(k_3)\left(k_1^2 - \frac{\omega_1^4}{g^2}\right)\cos\theta_{q3} - \frac{\omega_1^3}{g}\tanh qh\right]}{\left[\frac{g}{q}\tanh qh - C_g^2(k_3)\cos^2\theta_{q3}\right]} \\ & + \frac{1}{2}\left(k_3^2 - \frac{\omega_3^4}{g^2}\right)\left(k_1^2 - \frac{\omega_1^4}{g^2}\right) - \frac{2\omega_1^2\omega_3^2k_3^2}{g^2}. \end{aligned} \tag{31}$$

The denominator in this expression is always positive, as long as $q < k_3$. For infinite depth, only the final term remains, and the expression has a simple limiting value of $-\omega_1^2\omega_3^4/g^3$. For finite depth, however, $D_{\mathbf{k}_1\mathbf{k}_2-\mathbf{k}_3}^{+\ +\ -}$ depends on the approach directions θ_{q3} and θ_{q1}, from which $\mathbf{k}_2$ and $\mathbf{k}_4$ respectively approach $\mathbf{k}_3$ and $\mathbf{k}_1$. This results in a discontinuity at $\mathbf{k}_1 - \mathbf{k}_4 = \mathbf{k}_3 - \mathbf{k}_2 = \mathbf{0}$.

In the shallow-water limit,

$$D_{\mathbf{k}_1\mathbf{k}_2-\mathbf{k}_3}^{+\ +\ -} \xrightarrow[h\to 0]{} k_1^2k_3^2\left(\frac{3\cos\theta_{q3}\left(\cos\theta_{q1} + \frac{1}{2}\cos\theta_{q3}\right)}{\{1 - [1 - (k_3h)^2]\cos^2\theta_{q3} + O[(k_3h)^4]\}} + \frac{1}{2}\right), \tag{32}$$

so the difference between the maximum and minimum values of $D_{\mathbf{k}_1\mathbf{k}_2-\mathbf{k}_3}^{+\ +\ -}$ in the immediate vicinity of the discontinuity is proportional to $k_1^2/h^2 = \omega_1^2/(gh^3)$.

The second term $D_{\mathbf{k}_2-\mathbf{k}_3\mathbf{k}_1}^{+\ -\ +}$ also introduces a similar discontinuity (at $\mathbf{k}_1 - \mathbf{k}_3 = \mathbf{k}_4 - \mathbf{k}_2 = \mathbf{0}$), while the third term introduces discontinuities at $\mathbf{k}_1 = \mathbf{0}$ and $\mathbf{k}_2 = \mathbf{0}$. An example can be seen in Fig. 2, where the full interaction coefficient $D(\mathbf{k}_1, \mathbf{k}_2, \mathbf{k}_3, \mathbf{k}_4)$ is plotted as a function of the two components of the vector $\hat{\mathbf{k}} = \mathbf{k}_1 - ½(\mathbf{k}_3 + \mathbf{k}_4) = ½(\mathbf{k}_3 + \mathbf{k}_4) - \mathbf{k}_2$. In this example, $\mathbf{k}_3$ and $\mathbf{k}_4$ have been fixed, and the other wavenumbers $\mathbf{k}_1$ and $\mathbf{k}_2$ allowed to vary, constrained by the wavenumber resonance condition (4), but not by the frequency constraint (5). Wavenumber combinations that do satisfy the latter condition are represented by a solid line in Fig. 2. The line passes through the $\mathbf{k}_1 = \mathbf{k}_3$ and $\mathbf{k}_1 = \mathbf{k}_4$ discontinuities, but not those at $\mathbf{k}_1 = \mathbf{0}$ and $\mathbf{k}_2 = \mathbf{0}$ (except in the degenerate case $\mathbf{k}_1 = \mathbf{k}_2 = \mathbf{k}_3 = \mathbf{k}_4 = \mathbf{0}$). Solution of the nonlinear source term integral (2) requires the interaction coefficient to be evaluated along this line, which establishes the approach directions of relevance in the limiting case (31).

In order to calculate the orientation of the resonance line at an arbitrary point, suppose $\mathbf{k}_1$ is on the resonance curve, for some fixed $\mathbf{k}_3$ and $\mathbf{k}_4$. Then if this vector is shifted to $\mathbf{k}_1 + \boldsymbol{\varepsilon}$, with a corresponding shift of $\mathbf{k}_2$ to $\mathbf{k}_2 - \boldsymbol{\varepsilon}$, this will remain a valid solution if $\omega_1 + \omega_2 - \omega_3 - \omega_4$ remains zero. If the angle between $\boldsymbol{\varepsilon}$ and $\mathbf{k}_i$ is $\theta_{\varepsilon i} = \theta_\varepsilon - \theta_i$ (for $i = 1, 2, 3, 4$), then the change in ω_1 will be (Herterich and Hasselmann 1980)

$$\delta\omega_1 = C_g(k_1)\varepsilon\cos\theta_{\varepsilon 1} + \tilde{C}(k_1)\varepsilon^2\cos^2\theta_{\varepsilon 1} + \tilde{S}(k_1)\varepsilon^2\sin^2\theta_{\varepsilon 1} + O(\varepsilon^3), \qquad (33)$$

where C_g is the group velocity (8),

$$\tilde{C}(k) = \frac{1}{2}\frac{dC_g}{dk} = -\frac{g^2}{8\omega^2}\tanh^2 kh\left[\left(1 - \frac{2kh}{\sinh 2kh}\right)^2 + \left(\frac{2kh}{\cosh kh}\right)^2\right], \qquad (34)$$

and

$$\tilde{S}(k) = \frac{1}{2k}C_g = \frac{g^2}{4\omega^2}\tanh^2 kh\left(1 + \frac{2kh}{\sinh 2kh}\right). \qquad (35)$$

Adding in the corresponding change in ω_2 and requiring the total change in the wavenumber sum to cancel, we obtain

$$\begin{aligned} 0 &= \delta\omega_1 + \delta\omega_2 \\ &= C_g(k_1)\varepsilon\cos\theta_{\varepsilon 1} + \tilde{C}(k_1)\varepsilon^2\cos^2\theta_{\varepsilon 1} \\ &\quad + \tilde{S}(k_1)\varepsilon^2\sin^2\theta_{\varepsilon 1} - C_g(k_2)\varepsilon\cos\theta_{\varepsilon 2} \\ &\quad + \tilde{C}(k_2)\varepsilon^2\cos^2\theta_{\varepsilon 2} + \tilde{S}(k_2)\varepsilon^2\sin^2\theta_{\varepsilon 2} + O(\varepsilon^3). \end{aligned} \qquad (36)$$

If $\mathbf{k}_1 \neq \mathbf{k}_2$ we can ignore second- and higher-order terms, and find that

$$\begin{aligned} C_g(k_2)\cos\theta_{\varepsilon 2} &= C_g(k_1)\cos\theta_{\varepsilon 1} \\ &= C_g(k_1)[\cos\theta_{\varepsilon 2}\cos(\theta_2 - \theta_1) \\ &\quad - \sin\theta_{\varepsilon 2}\sin(\theta_2 - \theta_1)], \end{aligned} \qquad (37)$$

since $\theta_{\varepsilon 1} = \theta_{\varepsilon 2} + \theta_2 - \theta_1$. Hence the direction of allowed perturbations from $\mathbf{k}_2$ is given by

$$\tan\theta_{\varepsilon 2} = \frac{C_g(k_1)\cos(\theta_2 - \theta_1) - C_g(k_2)}{C_g(k_1)\sin(\theta_2 - \theta_1)}. \qquad (38)$$

This condition has two solutions, for the points on the resonance line either side of the initial point $\mathbf{k}_2$. The corresponding condition near $\mathbf{k}_1$ is

$$\tan\theta_{\varepsilon 1} = \frac{C_g(k_2)\cos(\theta_1 - \theta_2) - C_g(k_1)}{C_g(k_2)\sin(\theta_1 - \theta_2)}. \qquad (39)$$

The limiting value of $D^{++-}_{\mathbf{k}_1\mathbf{k}_2-\mathbf{k}_3}$ along the resonance solution line can then be found by setting $\mathbf{q} = \mathbf{k}_2 - \mathbf{k}_3 = \mathbf{k}_4 - \mathbf{k}_1 = \varepsilon$ and substituting

$$\cos^2\theta_{q3} = \cos^2\theta_{q2} = \cos^2\theta_{\varepsilon 2} = \frac{C_g^2(k_1)\sin^2(\theta_2 - \theta_1)}{C_g^2(k_1) - 2C_g(k_1)C_g(k_2)\cos(\theta_2 - \theta_1) + C_g^2(k_2)}, \quad \text{and} \qquad (40)$$

$$\cos^2\theta_{q1} = \cos^2\theta_{\varepsilon 1} = \frac{C_g^2(k_3)}{C_g^2(k_1)}\cos^2\theta_{\varepsilon 2} \qquad (41)$$

in Eq. (31). Because the direction enters as $\cos^2\theta$, $D^{++-}_{\mathbf{k}_1\mathbf{k}_2-\mathbf{k}_3}$ has the same finite limit from both directions and varies continuously along the resonance line through $\mathbf{k}_2 = \mathbf{k}_3$ (Fig. 2).

For the case $\mathbf{k}_1 = \mathbf{k}_2 = \mathbf{k}_3 = \mathbf{k}_4$, which is the only discontinuity considered by Herterich and Hasselmann (1980), the derivation given above for the orientation of the resonance line breaks down, because with $C_g(k_1) = C_g(k_2)$ and $\theta_{\varepsilon 1} = \theta_{\varepsilon 2}$ the first-order terms in (36) are zero for arbitrary angle. In this case, we need to retain the second-order terms, to find

$$\tilde{C}(k_1)\cos^2\theta_{\varepsilon 1} + \tilde{S}(k_1)\sin^2\theta_{\varepsilon 1} = 0, \qquad (42)$$

hence

$$\tan^2\theta_{\varepsilon 1} = -\frac{\tilde{C}(k_1)}{\tilde{S}(k_1)} = \frac{1}{2}\left[\left(1 - \frac{2k_1h}{\sinh 2k_1h}\right)^2 + \left(\frac{2k_1h}{\cosh k_1h}\right)^2\right] \times\left(1 + \frac{2k_1h}{\sinh 2k_1h}\right)^{-1}. \qquad (43)$$

This has four solutions, as the resonance line for the case $\mathbf{k}_3 = \mathbf{k}_4$ crosses itself at the origin. However, because $\cos^2\theta_{\varepsilon 1}$ is the same for each case, the interaction coefficient converges to the same limit (31) along each of the approach directions. The evaluation of the interaction coefficient along the integration path then presents no greater difficulties at this discontinuity than does the more general case.

In the narrow peak approximation derived by Herterich and Hasselmann (1980), this discontinuity is treated by averaging over the approach direction. The above results indicate that such an approach is both inaccurate and unnecessary, as only the values on the actual, well-defined approach directions are relevant.

The denominator term S of Eq. (11) vanishes at the center of the interaction diagram; indeed it does so whenever $\mathbf{k}_1 = \mathbf{k}_2 = ½\mathbf{k}_a$, for any combination of $\mathbf{k}_3$ and $\mathbf{k}_4$ lying on the same resonance curve, not just the special case $\mathbf{k}_1 = \mathbf{k}_2 = \mathbf{k}_3 = \mathbf{k}_4$. Examining this more

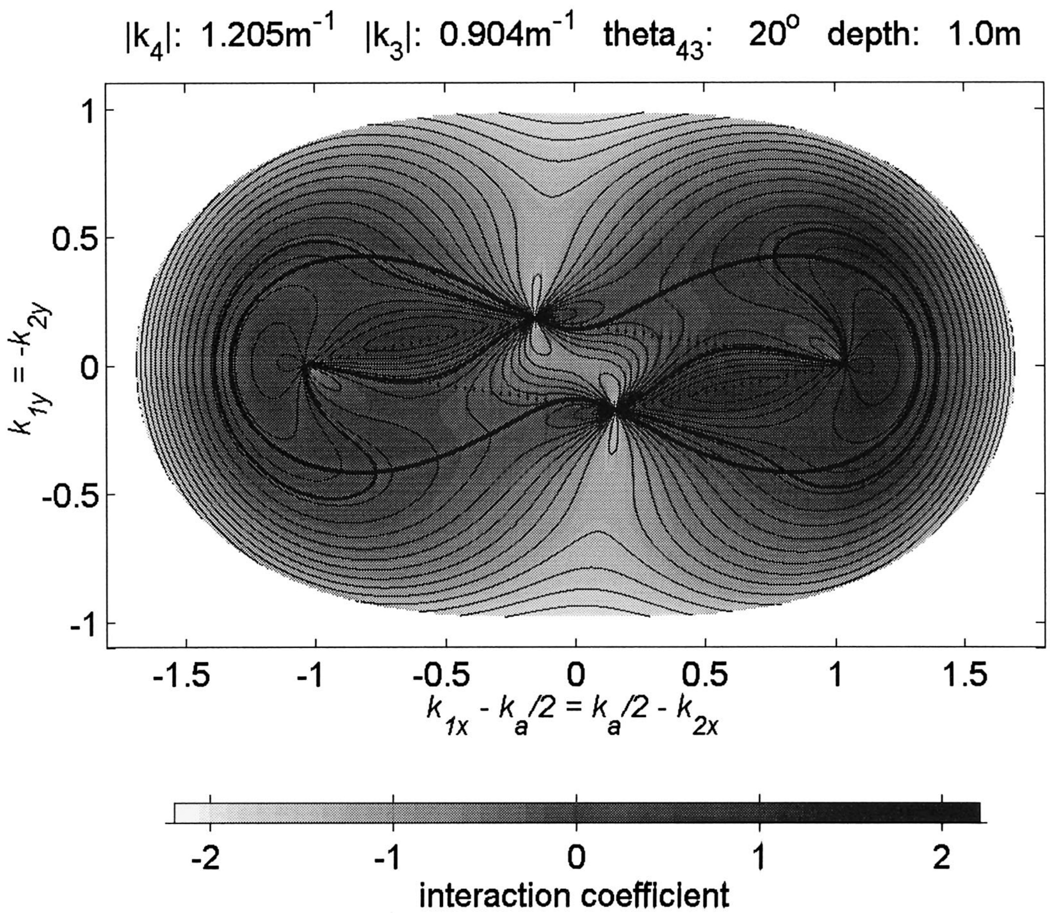

FIG. 2. Variation of the interaction coefficient $D(\mathbf{k}_1, \mathbf{k}_2, \mathbf{k}_3, \mathbf{k}_4)$ as a function of the two components of the vector $\hat{\mathbf{k}} = \mathbf{k}_1 - ½(\mathbf{k}_3 + \mathbf{k}_4) = ½(\mathbf{k}_3 + \mathbf{k}_4) - \mathbf{k}_2$. The zero contour is marked by a thicker line. In this example, the water depth is 1 m, and $\mathbf{k}_3$ and $\mathbf{k}_4$ are constant with magnitudes $k_3 = 0.904\ \mathrm{m}^{-1}$, $k_4 = 1.205\ \mathrm{m}^{-1}$, and directions differing by 20°. Wavenumbers $\mathbf{k}_1$ and $\mathbf{k}_2$ are constrained by the wavenumber resonance condition (4), but not by the frequency constraint (5). Wavenumber combinations that do satisfy the latter condition are represented by a solid line that passes through discontinuities at $\mathbf{k}_1 = \mathbf{k}_3(\mathbf{k}_2 = \mathbf{k}_4)$ and $\mathbf{k}_1 = \mathbf{k}_4(\mathbf{k}_2 = \mathbf{k}_3)$, and outside the discontinuities at $\mathbf{k}_1 = 0$ and $\mathbf{k}_2 = 0$.

general case by taking the limit of small $\boldsymbol{\varepsilon} = \mathbf{k}_1 - ½\mathbf{k}_a = ½\mathbf{k}_a - \mathbf{k}_2$, we note that

$$k_2 = \sqrt{k_1^2 - 4\mathbf{k}_1 \cdot \boldsymbol{\varepsilon} + 4\varepsilon^2}$$
$$= k_1 - 2k_1\varepsilon \cos\theta_{\varepsilon 1} + O(\varepsilon^2), \quad (44)$$

and hence, again using the group velocity gradient $\tilde{C}$ defined in (34),

$$C_g(k_2) = C_g(k_1) - 4\varepsilon k_1 \cos\theta_{\varepsilon 1}\tilde{C}(k_1) + O(\varepsilon^2). \quad (45)$$

We then find that S has a linear dependence on ε:

$$S = \left|1 - \frac{C_g(k_2)}{C_g(k_1)}\cos(\theta_2 - \theta_1)\right|$$
$$= \left|4\varepsilon \cos\theta_{\varepsilon 1}\frac{\tilde{C}(k_1)}{C_g(k_1)}\right| + O(\varepsilon^2), \quad (46)$$

in which we can again use the approach angle given by (39).

The methods for evaluating the integral (2) quoted in the literature (Hashimoto et al. 1998; Resio and Perrie 1991; Snyder et al. 1993) will generally have an internal loop where two of the wavenumbers (e.g., $\mathbf{k}_3$ and $\mathbf{k}_4$) have been fixed, and for successive values of the remaining free parameter, (e.g., the direction θ_1 of the vector $\mathbf{k}_1$), the other variables (e.g., k_1, k_2, θ_2) are set by the resonance conditions (4) and (5). Any roundoff error in evaluating these wavenumber parameters will result in the interaction coefficient being evaluated slightly off the resonance line. Near the discontinuities, this will result in a finite error in evaluating the interaction coefficient unless specific measures are made to ensure that the coefficient is evaluated on the resonance line by a method such as that described above.

The significance of these errors to the computation of the Boltzmann integral (7) will depend on the behaviour of the other terms, which we consider in the following section.

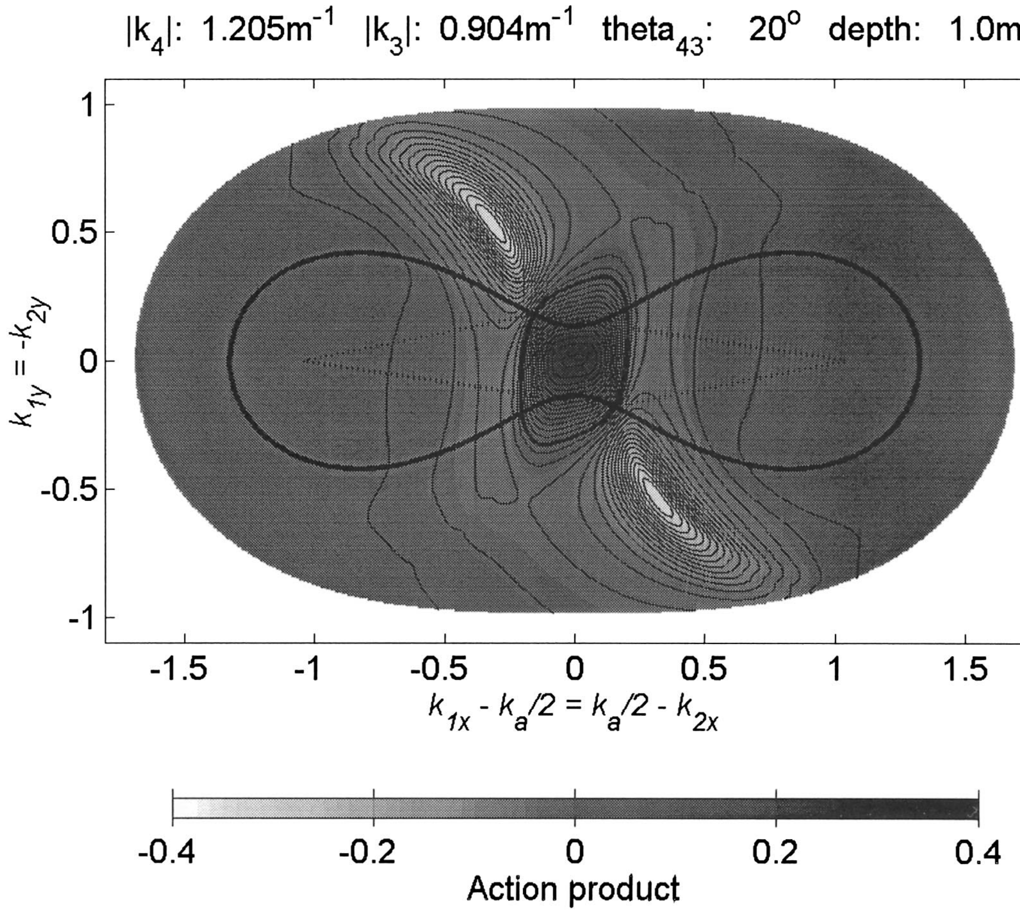

FIG. 3. Variation of the action product $N_{\mathrm{prod}} = N_1N_2(N_3 + N_4) - N_3N_4(N_1 + N_2)$ as a function of the two components of the vector $\hat{\mathbf{k}} = \mathbf{k}_1 - \frac{1}{2}(\mathbf{k}_3 + \mathbf{k}_4) = \frac{1}{2}(\mathbf{k}_3 + \mathbf{k}_4) - \mathbf{k}_2$, for the same case as shown in Fig. 2. The zero contour is marked by a thicker line. The action is derived from a JONSWAP spectrum with Mitsuyasu–Hasselmann directional spreading, with peak wavenumber $\mathbf{k}_p = 0.9\ \mathrm{m}^{-1}$ (marked by a +). Wavenumbers $\mathbf{k}_1$ and $\mathbf{k}_2$ are constrained by the wavenumber resonance condition (4), but not by the frequency constraint (5). Wavenumber combinations that do satisfy the latter condition are represented by a solid line.

4. Structure of the action product term

We can immediately see that the action product term

$$N_{\mathrm{prod}} = N_1N_2(N_3 + N_4) - N_3N_4(N_1 + N_2) \quad (47)$$

vanishes for ($\mathbf{k}_1 = \mathbf{k}_3$, $\mathbf{k}_2 = \mathbf{k}_4$) and for ($\mathbf{k}_1 = \mathbf{k}_4$, $\mathbf{k}_2 = \mathbf{k}_3$). In the neighborhood of one of these points, for example, for small $\mathbf{q} = \mathbf{k}_2 - \mathbf{k}_3 = \mathbf{k}_1 - \mathbf{k}_4$, we find $N_{\mathrm{prod}} = O(q)$ for the general case $\mathbf{k}_3 \neq \mathbf{k}_4$, while $N_{\mathrm{prod}} = O(q^2)$ for $\mathbf{k}_3 = \mathbf{k}_4$. This assumes that the action has a nonzero gradient in wavenumber space at both $\mathbf{k}_3$ and $\mathbf{k}_4$—otherwise there will be a higher-order q dependence. For the $\mathbf{k}_3 = \mathbf{k}_4$ case, from (44) we see that the S term in the denominator is linear in q, so the full integrand of the Boltzmann integral (7) vanishes as $O(q)$ at the critical points in either case.

As a result, errors in the evaluation of the interaction coefficient in the neighborhood of these points do not have any effect larger than the normal discretization error. This also suggests that a special "singularity" treatment such as that proposed by Masuda (1980) to integrate around the point $\mathbf{k}_1 = \mathbf{k}_2 = \mathbf{k}_3 = \mathbf{k}_4$ may not be necessary, although the more general case $\mathbf{k}_1 = \mathbf{k}_2 \neq \mathbf{k}_3 \neq \mathbf{k}_4$ where N_{prod} is nonzero will still need to be treated.

As we did previously for D, we now consider the behavior of N_{prod} for fixed $\mathbf{k}_3$ and $\mathbf{k}_4$, varying $\mathbf{k}_1$ and $\mathbf{k}_2$ subject to the wavenumber condition (4) but with the ω resonance condition (5) relaxed. Figure 3 shows this for the same choice of $\mathbf{k}_3$ and $\mathbf{k}_4$ as in Fig. 2. For illustrative purposes, an action function derived from a JONSWAP spectrum with Mitsuyasu–Hasselmann directional spreading has been used (Hasselmann et al. 1973; Mitsuyasu et al. 1975). The action product term has a zero contour passing through the two critical points $\mathbf{k}_1 = \mathbf{k}_3$ and $\mathbf{k}_1 = \mathbf{k}_4$. Inside this contour the product is positive, with a maximum at $\mathbf{k}_1 = \mathbf{k}_2 = \frac{1}{2}(\mathbf{k}_3 + \mathbf{k}_4) = \frac{1}{2}\mathbf{k}_a$. Outside the zero contour, there are two symmetrically placed minima, located near $\mathbf{k}_1 = \mathbf{k}_p$ and $\mathbf{k}_2 = \mathbf{k}_p$. Other details will also depend on the form of the action function, but the general form of N_{prod}, arising

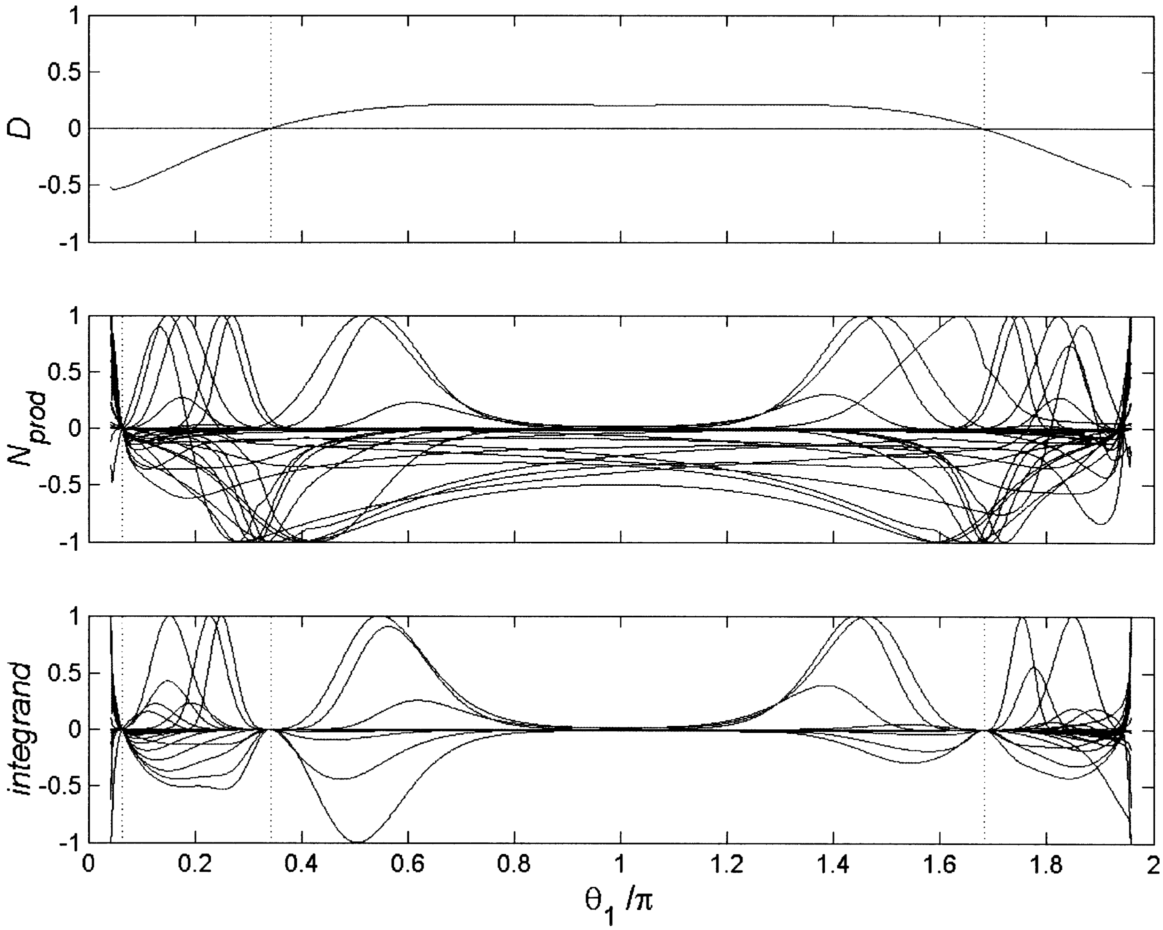

FIG. 4. Variation along the ω resonance line of (a) the interaction coefficient D, (b) the action product $N_{\rm prod} = N_1N_2(N_3 + N_4) - N_3N_4(N_1 + N_2)$, and (c) the integrand $\{[(k_1k_3)/C_g(k_1)C_g(k_3)]\ (G/S)\}[N_1N_2(N_3 + N_4) - N_3N_4(N_1 + N_2)]$ from the Boltzmann integral (7). The latter two functions are normalized by the maximum magnitude. Parameters are plotted as a function of θ_1, restricted to $|\mathbf{k}_1| < |\mathbf{k}_2|$, i.e., the left half of Fig. 1. In this example, the water depth is 1 m, and $\mathbf{k}_3$ and $\mathbf{k}_4$ are constant with magnitudes $k_3 = 0.904$ m^{-1}, $k_4 = 1.205$ m^{-1}, and directions differing by 20°. The action function is derived from a JONSWAP spectrum with Mitsuyasu–Hasselmann directional spreading, with each combination of peak wavenumber $\{k_p = 0.5, 1, 2$ m$^{-1}\}$ and peak direction $\{\theta_p = 0°, 30°, \ldots, 330°\}$. The location of fixed zeroes of D and $N_{\rm prod}$ are marked by dashed lines.

from the presence of a stationary point at ½$\mathbf{k}_a$ and of a zero contour passing through the critical points, is robust.

The effect of this consistent structure can be seen from Fig. 4, which shows D, $N_{\rm prod}$, and the full integrand of the Boltzmann integral (7) evaluated along the left half of the ω resonance line for a set of action functions based on JONSWAP spectra with Mitsuyasu–Hasselmann directional spreading, for a range of peak wavenumbers. This is not a particularly narrow-peaked spectral shape, but the action product varies considerably in magnitude around the resonance curve. It has zeroes at the critical point $\mathbf{k}_1 = \mathbf{k}_3$, and for at least one other point where the zero contour of $N_{\rm prod}$ crosses the interaction curve. In this case, the interaction coefficient has two zeroes in each half of the resonance line, so the D^2 term introduces two further second-order zeroes into the integrand. Like the critical point, these are at fixed positions independent of the action function.

5. Discussion

The presence of discontinuities in the interaction coefficient means that an algorithm to compute the Boltzmann integral (7) needs to take some care in their vicinity. The discontinuities are removed when the interacting wavenumbers are constrained to satisfy the resonance conditions, but they are of practical importance if numerical error allows the interaction coefficient to be evaluated for slightly ''nonresonant'' wavenumbers nearby. This can be avoided by the methods described above. However, the vanishing of the action product term at the corresponding points means that any error in evaluating the interaction coefficient should not produce an extra error in evaluating the Boltzmann integral. Nonlinear transfer rates computed by the EXACT-NL algorithm, for example, were found to be unaffected by correcting the interaction coefficient algorithm at the discontinuities.

Studies in which nonlinear transfer rates have been computed for shallow water (Snyder et al. 1993; Hashimoto et al. 1998) show unstable behavior, with possibly spurious fine structure. Snyder et al. (1993) found that an integration grid much finer than that used to represent the spectrum is needed to begin to produce stable results, and had great difficulty producing convergence. We have noted here that the interaction coefficient discontinuities increase in magnitude with decreasing depth. However, when properly restricted by the resonance conditions, the interaction coefficient shows relatively slow variation over the wavenumber domain for both deep and shallow water. So inadequate resolution of D should not be a limiting factor for accurate computation of S_{nl4} in shallow water.

The kernel of the Boltzmann integral does, however, pick up strong variation from the action product term as well as singular behaviour from the denominator term S. The resulting need for very fine grid resolution is problematic for such a high-dimension numerical computation, and it may be advantageous to consider more advanced quadrature algorithms that achieve a desired accuracy with fewer sampling points. As noted here, the kernel has a set of zeroes located independently of the details of the action density. It remains to be investigated whether this information can be usefully exploited in a numerical integration scheme. Two points of practical importance emerge from this analysis. First, the special treatment used by Masuda (1980) and Hashimoto et al. (1998) to integrate around the discontinuity in S may be unnecessarily cumbersome. Second, the narrow peak approximation as derived by Herterich and Hasselmann (1980) can be made more accurate by revising the method of averaging around the discontinuity.

Acknowledgments. This study was funded by the New Zealand Foundation for Research, Science and Technology (Wave and Sediment Dynamics in Coastal and Estuarine Systems, Contract CO1686). Murray Smith, Andrew Laing, Karin Bryan, and Gerbrant van Vledder contributed valuable comments on the contents of the paper.

APPENDIX

List of Symbols

$\tilde{C}$, $\tilde{S}$	Terms in Taylor series for $\delta\omega$
C_g	Wave group velocity
$D(\mathbf{k}_1, \mathbf{k}_2, \mathbf{k}_3, \mathbf{k}_4)$	Interaction coefficient
$D^{s_1 s_2 s_3}_{\mathbf{k}_1 \mathbf{k}_2 \mathbf{k}_3}$	Term in interaction coefficient
$D^{s_2 s_3}_{\mathbf{k}_2 \mathbf{k}_3}$	Term in interaction coefficient
$E^{s_2 s_3}_{\mathbf{k}_2 \mathbf{k}_3}$	Term in interaction coefficient
g	Gravitational acceleration
G	Interaction coefficient
h	Water depth
$\mathbf{k}$	Wavenumber vector
k	Magnitude of $\mathbf{k}$
$\mathbf{k}_1$, $\mathbf{k}_2$, $\mathbf{k}_3$, $\mathbf{k}_4$	Interacting wavenumber vectors
$\mathbf{k}_a$	$\mathbf{k}_3 + \mathbf{k}_4$
k_a	Magnitude of $\mathbf{k}_a$
k_p	Peak wavenumber
N_{prod}	Wave action product term
N_1, N_2, N_3, N_4	Interacting wave action densities
$\mathbf{q}$, $\boldsymbol{\varepsilon}$	Wavenumber difference vectors
S	Interaction term denominator
s_i	± 1
S_{in}, S_{nl3}, S_{diss}	Other source terms for spectral wave growth
S_{nl4}	Four-wave nonlinear interaction source term
t	Time
$\mathbf{x}$	Position vector
$\delta(x)$	Dirac delta function
Φ	Wave spectral density
π	3.14159 . . .
ρ	Water density
θ_1, θ_2, θ_3, θ_4	Interacting wave directions
θ_a	Direction of $\mathbf{k}_a$
θ_{q1}, θ_{q3}, $\theta_{\varepsilon 1}$, $\theta_{\varepsilon 2}$	Relative wave directions
Θ	Limit of wave direction integration range
ω	Wave angular frequency
ω_1, ω_2, ω_3, ω_4	Interacting wave angular frequencies
ω_{k_i}	$s_i \omega(\mathbf{k}_i)$

REFERENCES

Booij, N., R. C. Ris, and L. H. Holthuijsen, 1999: A third-generation wave model for coastal regions. 1. Model description and validation. *J. Geophys. Res.,* **104,** 7649–7666.

Gorman, R. M., and C. G. Neilson, 1999: Modelling shallow water wave generation and transformation in an intertidal estuary. *Coastal Eng.,* **36,** 197–217.

Hashimoto, N., H. Tsuruya, and Y. Nakagawa, 1998: Numerical computations of the nonlinear energy transfer of gravity-wave spectra in finite water depths. *Coastal Eng. J. (Japan),* **40,** 23–40.

Hasselmann, K., 1962: On the non-linear energy transfer in a gravity-wave spectrum. Part 1. General theory. *J. Fluid Mech.,* **12,** 481–500.

——, 1963: On the non-linear energy transfer in a gravity-wave spectrum. Part 2. Conservation theorems: Wave-particle analogy; irreversibility. *J. Fluid Mech.,* **13,** 273–281.

——, and Coauthors, 1973: Measurements of wind-wave growth and swell decay during the Joint North Sea Wave Project (JONSWAP). *Dtsch. Hydrogr. Z.,* **8** (12; Suppl. A), 1–95.

Hasselmann, S., and K. Hasselmann, 1985: Computations and parameterizations of the nonlinear energy transfer in a gravity wave spectrum. Part I: A new method for efficient computations of the exact nonlinear transfer integral. *J. Phys. Oceanogr.,* **15,** 1369–1377.

——, ——, J. H. Allender, and T. P. Barnett, 1985: Computations and parameterizations of the nonlinear energy transfer in a gravity wave spectrum. Part II: Parameterizations of the nonlinear energy transfer for application in wave models. *J. Phys. Oceanogr.,* **15,** 1378–1391.

——, and Coauthors, 1988: The WAM Model—A third generation ocean wave prediction model. *J. Phys. Oceanogr.,* **18,** 1775–1810.

Herterich, K., and K. Hasselmann, 1980: A similarity relation for the nonlinear energy transfer in a finite-depth gravity-wave spectrum. *J. Fluid Mech.,* **97,** 215–224.
Holthuijsen, L. H., N. Booij, and R. C. Ris, 1993: A spectral wave model for the coastal zone. *Proc. Second Int. Symp. on Ocean Wave Measurement and Analysis,* New Orleans, LA, ASCE, 630–641.
Komatsu, K., and A. Masuda, 1996: A new scheme of nonlinear energy transfer among wind waves: RIAM method—Algorithm and performance. *J. Oceanogr.,* **52,** 509–537.
Longuet-Higgins, M. S., 1976: On the nonlinear transfer of energy in the peak of a gravity-wave spectrum: A simplified model. *Proc. Roy. Soc. London,* **A347,** 311–328.
Masuda, A., 1980: Nonlinear energy transfer between wind waves. *J. Phys. Oceanogr.,* **10,** 2082–2092.
Mitsuyasu, H., F. Tasai, T. Suhara, S. Mizuno, M. Okhuso, T. Honda, and K. Rikiishi, 1975: Observations of the directional spectrum of ocean waves using a cloverleaf buoy. *J. Phys. Oceanogr.,* **5,** 750–760.
Resio, D. T., and W. Perrie, 1991: A numerical study of nonlinear energy fluxes due to wave–wave interactions. Part 1. Methodology and basic results. *J. Fluid Mech.,* **223,** 603–629.
——, J. H. Pihl, B. A. Tracy, and C. L. Vincent, 2001: Nonlinear energy fluxes and the finite depth equilibrium range in wave spectra. *J. Geophys. Res.,* **106,** 6985–7000.
Ris, R. C., L. H. Holthuijsen, and N. Booij, 1999: A third-generation wave model for coastal regions. 2. Verification. *J. Geophys. Res.,* **104,** 7667–7681.
Snyder, R. L., W. C. Thacker, K. Hasselmann, S. Hasselmann, and G. Barzel, 1993: Implementation of an efficient scheme for calculating nonlinear transfer from wave–wave interactions. *J. Geophys. Res.,* **98,** 14 507–14 525.
Thacker, W. C., 1982: Some computational problems of oceanography. *Finite Elements in Water Resources: Proceedings of the 4th International Conference, Hannover, Germany, June 1982,* Springer-Verlag, 6.49–6.58.
Webb, D. J., 1978: Nonlinear transfer between sea waves. *Deep-Sea Res.,* **25,** 279–298.
Zakharov, V., 1999: Statistical theory of gravity and capillary waves on the surface of a finite-depth fluid. *Eur. J. Mech. B/Fluids,* **18,** 327–344.